AMP-activated protein kinase alpha2 deficiency affects cardiac cardiolipin homeostasis and mitochondrial function.

Yoni Athéa, Benoît Viollet, Philippe Mateo, Delphine Rousseau, Marta Novotova, Anne Garnier, Sophie Vaulont, James R. Wilding, Alain Grynberg, Vladimir Veksler, et al.

AMPKa2 DEFICIENCY AFFECTS CARDIAC CARDIOLIPIN HOMEOSTASIS AND MITOCHONDRIAL FUNCTION

Yoni Athéa[a,b,c], Benoît Viollet[d,e,f,g], Philippe Mateo[a,b,c], Delphine Rousseau[h,b,c], Marta Novotova[i], Anne Garnier[a,b,c], Sophie Vaulont[d,e,f,g], James R. Wilding[a,b,c], Alain Grynberg[h,b,c], Vladimir Veksler[a,b,c], Jacqueline Hoerter[a,b,c], Renée Ventura-Clapier[a,b,c]

[a]Inserm, U769, Châtenay-Malabry, F-92296 France;

[b]Université Paris-Sud 11, Châtenay-Malabry, F-92296 France ;

[c]IFR-141, Châtenay-Malabry, F-92296 France;

[d]Institut Cochin, Département Endocrinologie Métabolisme et Cancer, Paris, F-75014 France ;

[e]Inserm, U567, Paris, F-75014 France ;

[f]CNRS, UMR 8104, Paris, F-75014 France ;

[g]Université Paris 5, Faculté de Médecine René Descartes, UM 3, Paris, F-75014 France ;

[h]INRA-UMR-1154, Châtenay-Malabry F-92296, France ;

[i]Institute of Molecular Physiology and Genetics, Slovak Academy of Sciences, 833 34 Bratislava, Slovak Republic;

Short title: AMPK deficiency alters cardiolipin homeostasis

Address for correspondence: R. Ventura-Clapier, INSERM U-769, Université Paris-Sud, 5 rue J6B Clément, F-92296 Châtenay-Malabry, France.

Tel.: (331)46.83.57.62.

Fax: (331)46.83.54.75.

E-mail: renee.ventura@u-psud.fr

Main text word count: 3880

AMP-activated protein kinase (AMPK) plays an important role in controlling energy homeostasis and is envisioned as a promising target to treat metabolic disorders. In the heart, AMPK is involved in short-term regulation and in transcriptional control of proteins involved in energy metabolism. Here, we investigated whether deletion of AMPKα2, the main cardiac catalytic isoform, alters mitochondrial function and biogenesis. Body weight, heart weight and AMPKα1 expression were similar in control littermate and AMPKa2$^{-/-}$ mice. Despite normal oxygen consumption in perfused hearts, maximal oxidative capacity, measured using saponin permeabilized cardiac fibers, was ≈30 % lower in AMPKa2$^{-/-}$ mice with octanoate, pyruvate or glutamate+malate but not with succinate as substrates, showing an impairment at complex-I of the respiratory chain. This effect was associated with a 25% decrease in mitochondrial cardiolipin content, the main mitochondrial membrane phospholipid that is crucial for complex-I activity, and by a 13% decrease in mitochondrial content of linoleic acid, the main fatty acid of cardiolipins. The decrease in cardiolipin content could be explained by mRNA down-regulation of rate limiting enzymes of both cardiolipin synthesis (CDS2) and remodeling (ALCAT1). These data reveal a new role for AMPKα2 subunit in the regulation of cardiac muscle oxidative capacity via cardiolipin homeostasis.

Keywords: AMPK, mitochondria, complex-I, respiration, cardiolipins, fatty acids

INTRODUCTION

AMP-activated protein kinase (AMPK) signaling pathway plays an important role in controlling energy homeostasis at the whole body level by responding to hormonal or nutrient signals in the central nervous system and peripheral tissues that modulate food intake and energy expenditure (1,2). AMPK is an ubiquitous serine/threonine protein kinase activated by pathological stimuli, such as oxidative damage, osmotic shock, hypoxia, and glucose deprivation, as well as by physiological stimuli such as exercise, muscle contraction, and by hormones including leptin and adiponectin (3). It exists in cells as a heterotrimeric complex composed of a catalytic subunit (α) and two regulatory subunits (β and γ). Two α subunit isoforms exist, α1 and α2, α2 being the chief isoform expressed in striated muscle, accounting for 70-80% of the total AMPK catalytic activity in this tissue (4,5). Activation of AMPK causes up-regulation of ATP-producing catabolic pathways and down-regulation of ATP-consuming processes (3,6). It is activated in response to decreased cellular energy charge (high AMP/ATP ratio) and is involved in regulating carbohydrate and fat metabolism (3,5). AMPK acutely modulates mitochondrial oxidative flux via phosphorylation of Acetyl CoA carboxylase (ACC), decreasing malonyl-CoA levels and increasing oxidative flux through the mitochondrial carnitine palmitoyl transferase 1 (CPT-1) (1-3,5). It also increases glucose transport (7) and stimulates glycolysis by activating phosphofructokinase 2 (8). As such it is envisioned as a promising target to treat metabolic disorders such as metabolic syndrome, obesity and type 2 diabetes.

Such patients have increased susceptibility to cardiovascular disorders. The role of AMPK in the heart is not fully understood. Whereas AMPK is activated during pressure overload and exercise induced hypertrophy (9,10), it mediates the antihypertrophic effects of adiponectin (11). AMPK is involved in regulating carbohydrate and fatty acid transport notably during cardiac ischemia and reperfusion (5,8,12,13). As the final steps of carbohydrate and lipid oxidation take place in mitochondria, it is very probable that this enzyme also plays a role in mitochondrial substrate oxidation pathways.

AMPK can also affect energy metabolism through changes in gene expression. It is involved in skeletal muscle adaptation to exercise by increasing the expression of the peroxisome proliferator activated-receptor γ -coactivator-1α (PGC-1α) and activating mitochondrial biogenesis but again nothing is known concerning cardiac muscle (14). The aim of the present study was to investigate the possible involvement of AMPK in the control of cardiac mitochondrial function and biogenesis using specific AMPKα2 deficient mice (15).

These mice exhibit normal echocardiographic and hemodynamic characteristics but have altered glucose metabolism and a worse metabolic adaptation to ischemia (16).

RESEARCH DESIGN AND METHODS

Animals

The generation of AMPKa2$^{-/-}$ mice has been described elsewhere (15). Ten month old male AMPKa2$^{-/-}$ (n= 27) and control (n=25) littermate mice were used. Animals were housed under temperature-controlled conditions (21°C) and had free access to water and to a standard mouse chow. All procedures were performed in accordance with the principles and guidelines established by the European Convention for the Protection of Laboratory Animals. Mice were sacrificed by lethal intraperitoneal injection of pentothal (150mg/kg), for mitochondrial respiration experiments and tissue storage. Left ventricular tissue was isolated, part of which was immediately used for mitochondrial function measurement and part of which was rapidly frozen and kept at –80° C.

Perfused Hearts

Additional mice were anesthetized with urethane (2g/kg). Hearts were quickly removed and retrogradely perfused at a constant flow of 2.5 ml/min in the isovolumic Langendorff perfused mode without pacing. They were first equilibrated with 11mmol/L glucose for 30 minutes and then, with 5mM glucose and 0.4mM oleate prebound to 1% BSA as substrates for 20 more minutes. Left ventricular pressure was monitored from a water-filled balloon introduced in the left ventricle. Oxygen consumption (QO_2) was calculated from the difference in oxygen content between incoming (aortic) and outcoming (pulmonary artery) perfusates (17).

Electron microscopy

Left ventricular wall and papillary muscles were quickly isolated in oxygenated buffered Krebs solution without calcium to avoid ischemia, and fixed with 2% glutaraldehyde as previously described (18). For stereological analysis, papillary muscles were used to ensure longitudinal sections, and 3 randomly selected levels separated by more than 50 microns were used. From randomly selected cardiomyocytes (12-14 myocytes from each animal) the volume density of organelles was estimated by the point counting method (18). The volume density Vv of the organelles was estimated as Vv = p/P (p is the number of the test points hitting the image of the cellular components, P is the number of all points falling on the cardiomyocytes).

Study of in situ mitochondrial respiration

Oxygen consumption measurements of saponin-skinned fibers from left ventricle have been described previously (19,20). Rates of respiration are given in µmoles O_2.min^{-1}.g dry $weight^{-1}$ (dw).

Two different experimental protocols were used based on substrate utilization pathways (Figure 1). The first protocol determined the sensitivity of mitochondrial respiration to various substrates in the presence of 2mmol/l ADP, by cumulative substrate addition as described previously (21). The second protocol was aimed at determining the dependency of respiration on external [ADP] and [creatine] (22), with glutamate+malate as substrates. Respiration through complex-III was designed according to (23).

Biochemical studies

Frozen tissue samples were weighed, homogenized in ice-cold buffer and enzyme activities were determined as described previously (24). Complex-I activity was measured in heart homogenized in ice-cold buffer containing Tris Base 10mmol/l (pH 7.2), sucrose 75mmol/l, mannitol 225mmol/l, EDTA 100µmol/l, and Triton-X100 0.1%. To measure NADH-CoQ reductase activity with decyl-ubiquinone as electron acceptor, samples were incubated in phosphate buffer 25mmol/l pH 7.5, BSA 2.5mg/ml, decyl-ubiquinone 100µmol/l at 30°C. Activity was reported as rotenone-insensitive decrease in NADH absorbance at 340nm. NADH-ferricyanide reductase activity was measured with ferricyanide as electron acceptor and the decrease in absorbance was followed at 410nm.

Real-Time Quantitative RT-PCR Analysis

Total muscle RNA was extracted using standard procedures. Real-time RT-PCR was performed using the SYBR®Green method on a LightCycler rapid thermal cycler (Roche Diagnostics) as previously described (25). Values of each gene were normalized to cycA mRNA content and then corrected for the amount of RNA relative to muscle weight. Primers are listed in Table 1.

Western Blot Analysis

Specific antibodies were used to measure the protein content of the oxoglutarate/malate carrier (OMC) (26) (kind gift from Thomas Scholz and Stacia Koppenhafer, University of Iowa, USA), AMPKa1 and AMPKa2 (Upstate Biotechnology Inc., Lake Placid, New York, USA) in control and AMPK$\alpha 2^{-/-}$ mice.

Mitochondrial isolation and cardiolipin quantification

Mitochondria were isolated from cardiac ventricles of control and AMPKa$2^{-/-}$ mice according to Moreno-Sanchez et al (27). Cardiolipin was quantified by the spectrophotometric

method of Petit et al (28), using the high affinity of 10*N*-nonyl acridine orange (NAO) for cardiolipin of freshly isolated mitochondria.

Fatty Acid Composition

Lipids were extracted from heart, isolated cardiac mitochondria, liver and plasma in 2:1 chloroform-methanol. Phospholipids were separated from non-phosphorous lipids on silica acid cartridges, and fatty acids were *trans*-methylated with BF_3-methanol. Methyl esters were analyzed by gas chromatography on an Econo-cap EC-WAX capillary column (0.32x30m, Alltech Associates) coupled to a flame ionization detector using C17:0 as the internal standard as previously described (29).

Statistical analysis

Data are expressed as mean ± SEM. Student's t-test was used to determine the statistical significance of differences between group means. Statistical significance was defined as $P<0.05$.

RESULTS

General characteristics and base-line cardiac function

AMPKa2$^{-/-}$ mice had normal body (32±1 in control *versus* 37±3 g) and heart (187±8 in control *versus* 197±16 mg) weights, indicating that cardiac atrophy or hypertrophy were not present. Neither left ventricular pressure, or heart rate, or oxygen consumption of isolated hearts differed between control and AMPKα2$^{-/-}$ mice whether glucose, or glucose+oleate where used as substrates, suggesting that AMKPα2 deficiency does not alter cardiac work during normal perfusion (Table 2).

AMPKa1 protein content (as measured by Western blotting, not shown) was the same in control and AMPKa2$^{-/-}$ mice (1.24±0.12 in control versus 1.49±0.21 a.u.). Thus the deficiency in AMPKa2 was not compensated for by AMPKa1 overexpression.

Ultrastructure of the cardiomyocytes

In control cardiomyocytes, mitochondria formed longitudinal rows under sarcolemma and between myofibrils (Figures 2A and 2B). In contrast, in AMPKα2$^{-/-}$ cardiomyocytes from both papillary and ventricular muscles, splitting of myofibrils was frequently observed (Figure 2C-F). No change in total mitochondrial volume was observed (Table 3), but mitochondria lost their ellipsoid shape and became irregular in size (Figures 2C-F). They lost their arrangement in longitudinal rows and formed large and spread clusters especially under the sarcolemma (2D and 2F), so that the volume density of subsarcolemmal mitochondria was

increased (SS) while that of intermyofibrillar mitochondria (IM) was decreased (Table 3). No change in the volume of lipid droplets was observed (0.97±0.22 in control versus 0.79±0.61 %).

Cardiac mitochondrial function

Respiration rates for almost all substrates were significantly lower in cardiac fibers of AMPKα2$^{-/-}$ mice (Figure 3A). Compared to controls, respiration was decreased by 35% with malate, 34% following addition of octanoyl-carnitine, 38% after addition of pyruvate and 31% after final addition of glutamate in AMPKa2$^{-/-}$ mice, but did not change with glycerol-3-phosphate (G3P).

Respiration in the presence of phosphate acceptors, ADP and creatine, was studied with glutamate+malate (Vglu+mal) as substrates (Table 3). Basal respiration rate (V_0) and acceptor control ratio (ACR=Vglu+mal/V_0) were similar in control and AMPKa2$^{-/-}$ cardiac fibers. No difference was observed between the two groups for the affinity for ADP with or without creatine. The maximal oxygen-consumption rate was again 24% lower with glutamate+malate in the AMPKa2$^{-/-}$ mice (Table 3 and Figure 3). To determine at which point the respiratory chain was altered in AMPKa2$^{-/-}$ mice, complex-I was inhibited by amobarbital and respiration through complex-II was measured with succinate (Vsuc). Under succinate, no significant difference between the two groups was observed, whereas the ratio between complex-I- and complex-II-stimulated respiration (Vsuc/Vglu+mal) was increased by 42% in AMPKa2$^{-/-}$ mice (Table 3 and Figure 3B). No difference was observed for complex-III activated respiration with duroquinol (Vduroq). Thus, AMPKα2 deficiency induces a defect in mitochondrial respiration that appears limited to complex-I.

Energy metabolism enzymes

In order to understand the origin of mitochondrial defects, activities of key enzymes of energy metabolism were assessed (Table 3). Activity of citrate synthase, an index of mitochondrial mass, was similar in the two groups of mice. Other enzymes of the energy metabolism, total creatine kinase (CK), mitochondrial (mi-CK), adenylate kinase, total lactate dehydrogenase (LDH), and cytochrome c oxidase (COX) activities also remained unchanged in AMPKa2$^{-/-}$. Despite decreased respiration through complex-I, maximal complex-I and complex-II activities determined in tissue extracts were the same in both groups. To ensure that maximal complex-I activity was preserved in AMPKa2$^{-/-}$, we measured its activity using different electron acceptors, but no difference between the two groups was observed suggesting that AMPK deficiency did not affect mitochondrial enzyme content.

In an attempt to understand the origin of the decreased respiration through complex-I, malate-aspartate shuttle enzymes were measured (Table 3). Total malate dehydrogenase (MDH), mitochondrial MDH and the amount of OMC (6.8±1.2 (n=6) in control versus 5.1±0.5 a.u. in AMPKα2$^{-/-}$ (n=6), not shown) were unchanged in AMPKα2 deficient mice. Moreover, the mRNA levels of PGC-1α, the main regulator of mitochondrial biogenesis was similar in AMPKα2$^{-/-}$ and control hearts (Figure 4B), consistent with the preserved mitochondrial enzyme activities.

Cardiolipins and fatty acid composition

Complex-I activity *in situ* is critically dependent on the cardiolipin environment (30,31). In AMPKa2$^{-/-}$ mice, the amount of cardiolipin was 25% lower than in controls (Figure 4A). In addition, as evidenced in Table 4, the fatty acid composition of whole heart phospholipids and of isolated cardiac mitochondria in the AMPKa2$^{-/-}$ mice showed a significant decrease in linoleic acid proportion (~80 % of cardiolipin fatty acids). Conversely, linoleic acid was significantly increased in the non-phosphorous lipid fraction (which mainly contains storage triacylglycerol) of the whole heart homogenate. This decrease in linoleic acid content was specific to the heart since it neither decreased in liver phospholipids (19.4±0.8% and 19.6±1.1%, control versus AMPKa2$^{-/-}$) nor in plasma lipids (31.3±0.4% and 27.8±2.2%, respectively).

The level of expression of enzymes involved in cardiolipin homeostasis was determined (Figure 4B). Levels of CDS2, the enzyme that catalyzes the initial key step of cardiolipin synthesis, i.e. the conversion of phosphatidic acid to CDP-diacylglycerol, as well as of ALCAT1, an acyl-CoA:lysocardiolipin acyltransferase implicated in rapid cardiolipin remodeling (32,33), were significantly decreased in AMPKα2$^{-/-}$ mice while mRNA content of taffazin (TAZ), another phospholipid acyltransferase was unchanged. Interestingly, expression of CPT-1, the mitochondrial middle- and long-chain fatty acid transporter, was also significantly decreased in AMPK deficient mice.

DISCUSSION

The main results of this study can be summarized as follows. 1) Specific deficiency in AMPKα2 catalytic subunit did not induce cardiac atrophy or hypertrophy. 2) Oxygen consumption of isolated perfused heart was normal but mitochondrial ultrastructure was altered. 3) AMPK deficiency induced a decrease in maximal oxidative capacity of the cardiac muscle, whether lipids, pyruvate or glutamate+malate were used as substrates. 4) This was not

accompanied by changes in mitochondrial enzyme activities, the malate/aspartate shuttle or isolated complex-I or II *in vitro* activities. 5) When succinate was used as substrate, mitochondrial respiration was normal in AMPKa2$^{-/-}$ cardiac fibers, suggesting a defect in complex-I function *in situ*. 6) Cardiolipin content of AMPKa2$^{-/-}$ cardiac mitochondria was decreased by 25%, consistent with the altered ultrastructure and the functional defect of mitochondrial respiration by complex-I. 7) This defect was accompanied by a significant decrease in linoleic acid content of mitochondrial phospholipids and 8) could be explained by the decrease in the expression of key enzymes of cardiolipin biosynthesis and remodeling. Altogether these results suggest that AMPKα2 is involved in the control of mitochondrial respiration through cardiolipin homeostasis.

AMPKα2$^{-/-}$ mice exhibit perturbation in whole body insulin sensitivity, probably modulated by the sympathetic nervous system (15). These mice show normal cardiac content in AMPKα1 isoform suggesting that remnant AMPKα1 is unable to compensate for the lack of AMPKα2 (16).

A role for AMPK in controlling cardiac weight is still controversial. While AMPK was suggested to play a role in pressure overload hypertrophy (9), it was recently reported that adiponectin blocks cardiac hypertrophy by an AMPK dependent mechanism (11). Hearts of mice expressing of a dominant negative mutant of AMPKα2 exhibiting a residual AMPKα2 activity have preserved weight and baseline function (13). In another model, overexpressing a kinase-dead rat α2 isoform, the α2 protein content and activity were absent, and α1 content and activity were also decreased, the remnant α1 activity being attributed to endothelial cells (12). These mice exhibit a slightly decreased cardiac weight and contractility. However, we show here that AMPKα2$^{-/-}$ mice had normal cardiac weight. This suggests that the α2 subunit by itself is not essential for cardiac growth.

Oxygen consumption and contractile function were not different under basal conditions either with glucose or glucose plus oleate as substrates, as already described with glucose and pyruvate (16) in this mouse line. In KD mutant mice, cardiac function is slightly depressed at baseline (12). This difference could be due to the decreased AMPKa1 activity in this line. However, the workload of hearts perfused in the Langendorff mode is significantly less than in the working mode or *in vivo* and oxygen consumption does not reach maximal capacity.

To assess maximal mitochondrial function, respiration rates were measured in skinned fibers with saturating amounts of substrates, oxygen and phosphate acceptor. Depending upon

available substrates and cardiac demand, mitochondria are able to use acetyl-CoA produced from pyruvate by pyruvate dehydrogenase downwards of glycolysis, and/or acetyl-CoA produced by the β-oxidation of fatty acids, which enters the Krebs cycle (Figure 1). Mitochondria can also slightly use G3P by mitochondrial glycerophosphate dehydrogenase, which produces $FADH_2$ that enters the respiratory chain directly at the level of complex-II (34). We found a clear decrease in the respiration rate of AMPKa2$^{-/-}$ cardiac fibers, whether carbohydrate- or lipid-derived substrates were used. This suggests that AMPKα2 is involved in the control of cardiac oxidative capacity and in mitochondrial substrate utilization. Decreased energy availability in AMPKa2$^{-/-}$ mice would probably occur only at maximal workloads, so that the mitochondrial alterations observed here might be more evident during heavy exercise or under pathologic stress.

In order to understand the decrease in respiration of cardiac fibers, we looked at indicators of mitochondrial activity. In AMPKa2$^{-/-}$ mouse heart, levels of CS, a marker of mitochondrial mass, of COX, an enzyme of the respiratory chain, of mitochondrial creatine kinase (mi-CK), a phosphotransfer kinase, and of markers of the malate/aspartate shuttle, involved in glutamate+malate utilization, were normal. Additionally, PGC-1α, that induces mitochondrial biogenesis (35), and total mitochondrial volume density were unchanged as was also observed in skeletal muscles of mice with dominant negative mutant of AMPK (36). All this suggests that AMPKα2 is not essential for determining and maintaining mitochondrial mass in skeletal and cardiac muscle. However, it may play a role in cardiac mitochondrial biogenesis induced by external stimulus as was observed in skeletal muscle in response to exercise or chronic energy depletion (36).

Mitochondrial function also depends on the sensitivity to ADP and to creatine, the final acceptor of high-energy phosphates in cardiac mitochondria (37). No change in the sensitivity of respiration to ADP and creatine was observed, showing that the efficiency of cardiac mitochondria in phosphorylating ADP and producing phosphocreatine was not affected by AMPKα2 loss.

In order to explain the decreased respiration with preserved enzyme activities, we compared the respiration rates during activation from complex-I, or -II or -III (Figure 1 and 3, Table 2). Respiration with glutamate+malate mainly produces NADH that activates respiration through complex-I, while succinate oxidation mainly produces $FADH_2$ that is further oxidized by complex-II. Compared with controls, respiration was lower in AMPKa2$^{-/-}$ mice with glutamate+malate, but was normal with succinate, revealing an inhibition of

complex-I in these animals. Interestingly, respiration from G3P, which produces only $FADH_2$, was normal in AMPKa2$^{-/-}$ mice, while it was decreased for NADH producing substrates: pyruvate, octanoyl-carnitine. Moreover, respiration through complex-III was unchanged in AMPKα2$^{-/-}$ mice.

Despite a 24% decrease in respiration rate through complex-I, complex-I activity measured in total heart extracts was normal in AMPKa2$^{-/-}$ mice, independent of the electron acceptor. This indicated that the activity of isolated complex-I was not affected by AMPKa2 deficiency, suggesting an alteration of the *in situ* regulation of complex-I by cardiolipin. Indeed, activity of the complexes of the respiratory chain, and particularly of complex-I, strongly depends on the surrounding phospholipid environment of the inner mitochondrial membrane. Cardiolipin is the main functional phospholipid of the mitochondrial inner membrane, being present almost exclusively in mitochondria and representing 8-15% of the entire cardiac phospholipid mass. A 25% lower mitochondrial cardiolipin content was observed in AMPKa2$^{-/-}$ mice. Cardiolipin content is critical for the adaptation of energy metabolism to demand. It rises with increased metabolic rate or muscle performance (38), and plays a key role in the activity of several inner membrane proteins including complex-I (for review see (39)). Both complex-I and III were shown to require cardiolipin but, while being necessary for full complex-I activity (40), cardiolipin plays a structural rather than catalytic role for complex-III (41). Accordingly, respiration through complex-I but not complex-III was decreased in AMPK$\alpha_{2-/-}$ mice. Interestingly, in CHO cells, similar decrease in cardiolipin content induces similar alteration in complex-I activity in the respiratory chain without changes in isolated, complex-II, complex-III and IV and NADH-reductase activity (31). Mitochondrial creatine kinase binding in the vicinity of translocase is dependent on cardiolipin environment (42). It is possible that the rather small decrease in cardiolipin observed here was not sufficient to affect mi-CK function and activity.

Examination of cardiac ultrastructure of AMPKα2$^{-/-}$ mice revealed abnormal structure of mitochondria of various sizes, arranged in clusters under the sarcolemma and less in regular rows between myofilaments as in control hearts. While unchanged total mitochondrial volume was in accordance with preserved mitochondrial enzyme activity and PGC-1α expression, partial relocation of mitochondria from myofibrillar to subsarcolemmal space occurred. No evidence of ultrastructural changes was observed in AMPK KD mutant (12). However, in the present study these morphological changes were observed at higher magnification and could be more pronounced in older animals. Similarly in CHO cells, an

alteration of mitochondrial ultrastructure is specifically associated with reduction in cardiolipin content (31). Moreover, although to a lower extent, this resembles the ultrastructural abnormalities of mitochondria in the Barth syndrome, an X-linked disease. This disease, due to mutations in the tafazzin gene that belongs to the superfamily of phospholipid acyltransferase, is characterized by a dramatic reduction in cardiolipin content, and by abnormal mitochondrial ultrastructure (43).

Cardiolipin is the only phospholipid with four acyl chains, ~80% of which are composed of linoleic acid (18:2ω6), a polyunsaturated fatty acid of the ω6 series. The decrease in cardiolipin content in AMPKα2$^{-/-}$ heart was accompanied by a significant decrease in linoleic acid content of mitochondrial and whole heart phospholipids. The decrease in mitochondrial membrane linoleic acid observed in this study is neither due to nutritional differences since animals received the same chow diet, nor to a systemic effect since the plasma and liver lipid composition was unchanged. The fact that (i) the linoleic acid decrease parallels the cardiolipin decrease, (ii) cardiolipin contains approximately 80% linoleic acid, and (iii) the linoleic acid content in storage lipids was higher, suggests that the decrease in linoleic acid is a consequence rather than a cause of the cardiolipin decrease in AMPKα2 deficient mice. The lower linoleic acid content in heart compared to liver of AMPKα2$^{-/-}$ mice could be related to the higher proportion of AMPKα1 in liver (4). These animals are thus characterized by a dysfunction of cardiac cardiolipin homeostasis that affects the inner mitochondrial membrane and that could be the key effector of mitochondrial dysfunction.

Similar decreases in cardiolipin content and complex-I activity were reported following partial inhibition of cardiolipin synthesis in CHO cells (31). One important rate-limiting step of *de novo* cardiolipin synthesis is the initial reaction catalyzed by CTP:PA cytidylyltransferases (also called CDS) (33). In AMPKα2$^{-/-}$ mice expression of CDS2, the only cardiac isoform (44) is decreased, possibly explaining the decrease in cardiolipin content. A second mechanism of cardiolipin biosynthesis is through deacylation-reacylation which is catalyzed by phospholipases and acyltransferases, that are regarded as the principal enzymes involved in phospholipid remodeling in mammalian tissues (33). The acyltransferase ALCAT1 is regulated in concert with the level of cardiolipin and cardiolipin biosynthesis in mammalian heart (32,45). ALCAT1 mRNA expression was decreased in AMPKα2$^{-/-}$ mice like both CDS2 mRNA and cardiolipin content. All this suggests that AMPK is involved in cardiolipin homeostasis at least at the transcriptional level. Finally, expression of the

mitochondrial fatty acid transporter CPT-1 was also decreased in AMPKα2 deficient mice. Decreased activation of CPT-1 due to the lack of AMPK-modulated regulation of malonyl CoA content, together with the down-regulation of CPT-1, would have an additive inhibitory effect on fatty acid oxidation in AMPKα2$^{-/-}$ mice.

In summary, selective deficiency of AMPKα2 causes a significant decrease in maximal mitochondrial respiration, whether carbohydrates or lipids were used as substrates. This is due to a defect in the function of complex-I of the respiratory chain within the inner mitochondrial membrane, probably due to the decrease in cardiolipin content. Interestingly, it has been recently reported that the diabetic heart, characterized by altered lipid homeostasis and mitochondrial dysfunction, exhibit a dramatic decrease in cardiolipin content (46). These findings suggest that AMPK plays a critical role in the control of cardiac phospholipid homeostasis, possibly by modulating their metabolism through transcriptional machinery. More work is needed to elucidate the precise mechanisms by which AMPK may enhance energy production by favoring cardiolipin synthesis and thus improving the efficiency of the respiratory chain.

ACKNOWLEDGMENTS

We thank Dr. R. Fischmeister for continuous support. R.V.-C. is supported by the « Centre National de la Recherche Scientifique ». This work was supported by the “Association Française contre les Myopathies” and “Fondation de France”, the European Commission FP6 program (EXGENESIS-Grant QLG1-CT-2001-01488), and the European Union Contract (LSHM-CT-2005-018833/EUGeneHeart). The Franco-Slovak collaboration was funded by a French STEFANIK grant and by Slovak VEGA 2/6079/26 and APVT-51-31104. We thank J. Degrouard and D. Jaillard from the Centre Commun de Microscopie Electronique, Université Paris XI, Orsay and D. Fortin for skilful technical assistance.

REFERENCES

1. Kahn BB, Alquier T, Carling D & Hardie DG : AMP-activated protein kinase: ancient energy gauge provides clues to modern understanding of metabolism. *Cell Metab* 1:15-25, 2005

2. Fryer LG & Carling D: AMP-activated protein kinase and the metabolic syndrome. *Biochem Soc Trans* 33:362-666, 2005

3. Hardie DG, Scott JW, Pan DA & Hudson ER: Management of cellular energy by the AMP-

activated protein kinase system. *Febs Lett* 546:113-120, 2003

4. Cheung PC, Salt IP, Davies SP, Hardie DG & Carling D: Characterization of AMP-activated protein kinase gamma-subunit isoforms and their role in AMP binding. *Biochem J* 346:659-669, 2000

5. Sambandam N & Lopaschuk GD: AMP-activated protein kinase (AMPK) control of fatty acid and glucose metabolism in the ischemic heart. *Prog Lipid Res* 42:238-256, 2003

6. Hue L, Beauloye C, Bertrand L, Horman S, Krause U, Marsin AS, Meisse D, Vertommen D & Rider MH: New targets of AMP-activated protein kinase. *Biochem Soc Trans* 31:213-215, 2003

7. Russell RR 3rd, Bergeron R, Shulman GI & Young LH: Translocation of myocardial GLUT-4 and increased glucose uptake through activation of AMPK by AICAR. *Am J Physiol* 277:H643-H649, 1999

8. Marsin AS, Bertrand L, Rider MH, Deprez J, Beauloye C, Vincent MF, Van den Berghe G, Carling D & Hue L: Phosphorylation and activation of heart PFK-2 by AMPK has a role in the stimulation of glycolysis during ischaemia. *Curr Biol* 10:1247-1255, 2000

9. Tian R, Musi N, D'Agostino J, Hirshman MF & Goodyear LJ: Increased adenosine monophosphate-activated protein kinase activity in rat hearts with pressure-overload hypertrophy. *Circulation* 104:1664-1669, 2001

10. Coven DL, Hu X, Cong L, Bergeron R, Shulman GI, Hardie DG & Young LH: Physiologic Role of AMP-Activated Protein Kinase (AMPK) in the Heart: Graded Activation During Exercise. *Am J Physiol Endocrinol Metab* 285:E629-E636, 2003

11. Shibata R, Ouchi N, Ito M, Kihara S, Shiojima I, Pimentel DR, Kumada M, Sato K, Schiekofer S, Ohashi K, Funahashi T, Colucci WS & Walsh K: Adiponectin-mediated modulation of hypertrophic signals in the heart. *Nat Med* 10:1384-9, 2004

12. Russell RR 3rd, Li J, Coven DL, Pypaert M, Zechner C, Palmeri M, Giordano FJ, Mu J, Birnbaum MJ & Young LH: AMP-activated protein kinase mediates ischemic glucose uptake and prevents postischemic cardiac dysfunction, apoptosis, and injury. *J Clin Invest* 114:495-503, 2004

13. Xing Y, Musi N, Fujii N, Zou L, Luptak I, Hirshman MF, Goodyear LJ & Tian R: Glucose metabolism and energy homeostasis in mouse hearts overexpressing dominant negative alpha 2 subunit of AMP-activated protein kinase. *J Biol Chem* 278:28372-28377, 2003

14. Reznick RM & Shulman GI: The Role of AMP-Activated Protein Kinase in Mitochondrial Biogenesis. *J Physiol* 574:33-39, 2006

15. Viollet B, Andreelli F, Jorgensen SB, Perrin C, Geloen A, Flamez D, Mu J, Lenzner C, Baud O, Bennoun M, Gomas E, Nicolas G, Wojtaszewski JF, Kahn A, Carling D, Schuit FC, Birnbaum MJ, Richter EA, Burcelin R & Vaulont S: The AMP-activated protein kinase alpha2 catalytic subunit controls whole-body insulin sensitivity. *J Clin Invest* 111:91-98, 2003

16. Zarrinpashneh E, Carjaval K, Beauloye C, Ginion A, Mateo P, Pouleur AC, Horman S, Vaulont S, Hoerter JA, Viollet B, Hue L, Vanoverschelde JL & Bertrand L: Role of the alpha2 isoform of AMP-activated protein kinase in the metabolic response of the heart to no-flow ischemia. *Am J Physiol Heart Circ Physiol* 291:H2875-H2883, 2006

17. Hoerter J, Gonzalez Barroso MD, Couplan E, Mateo P, Gelly C, Cassard Doulcier AM, Diolez P & Bouillaud F: Mitochondrial uncoupling protein 1 expressed in the heart of transgenic mice protects against ischemic-reperfusion damage. *Circulation* 110:528-533, 2004

18. Novotova M, Pavlovicova M, Veksler V, Ventura-Clapier R & Zahradnik I: Ultrastructural remodeling of fast skeletal muscle fibers induced by invalidation of creatine kinase. *Am J Physiol Cell Physiol* 291:C1279-C1285, 2006

19. Veksler VI, Kuznetsov AV, Sharov VG, Kapelko VI & Saks VA: Mitochondrial respiratory parameters in cardiac tissue: a novel method of assessment by using saponin-skinned fibers. *Biochim Biophys Acta* 892:191-196, 1987

20. Saks VA, Veksler VI, Kuznetsov AV, Kay L, Sikk P, Tiivel T, Tranqui L, Olivares J, Winkler K, Wiedemann F & Kunz WS: Permeabilized cell and skinned fiber techniques in studies of mitochondrial function in vivo. *Mol Cell Biochem* 184:81-100, 1998

21. Bahi L, Koulmann N, Sanchez H, Momken I, Veksler V, Bigard AX & Ventura-Clapier R: Does ACE inhibition enhance endurance performance and muscle energy metabolism in rats? *J Appl Physiol* 96:59-64, 2004

22. Veksler VI, Kuznetsov AV, Anflous K, Mateo P, van Deursen J, Wieringa B & Ventura-Clapier R: Muscle creatine kinase-deficient mice.2. Cardiac and skeletal muscles exhibit tissue-specific adaptation of the mitochondrial function. *J Biol Chem* 270:19921-19929, 1995

23. Ray S, Dutta S, Halder J & Ray M: Inhibition of electron flow through complex I of the mitochondrial respiratory chain of Ehrlich ascites carcinoma cells by methylglyoxal. *Biochem J* 303:69-72, 1994

24. De Sousa E, Veksler V, Minajeva A, Kaasik A, Mateo P, Mayoux E, Hoerter J, Bigard X, Serrurier B & Ventura-Clapier R: Subcellular creatine kinase alterations - Implications in heart failure. *Circ Res* 85:68-76, 1999

25. Garnier A, Fortin D, Delomenie C, Momken I, Veksler V & Ventura-Clapier R: Depressed mitochondrial transcription factors and oxidative capacity in rat failing cardiac and skeletal muscles. *J Physiol* 551:491-501, 2003

26. Scholz TD, Koppenhafer SL, TenEyck CJ & Schutte BC: Developmental regulation of the alpha-glycerophosphate shuttle in porcine myocardium. *J Mol Cell Cardiol* 29:1605-1613, 1997

27. Moreno-Sanchez R & Hansford RG: Dependence of cardiac mitochondrial pyruvate dehydrogenase activity on intramitochondrial free Ca2+ concentration. *Biochem J* 256:403-412, 1988

28. Petit JM, Maftah A, Ratinaud MH & Julien R: 10N-nonyl acridine orange interacts with

cardiolipin and allows the quantification of this phospholipid in isolated mitochondria. *Eur J Biochem* 209:267-273, 1992

29. Rousseau D, Helies Toussaint C, Moreau D, Raederstorff D & Grynberg A: Dietary n-3 PUFAs affect the blood pressure rise and cardiac impairments in a hyperinsulinemia rat model in vivo. *Am J Physiol* 285:H1294-H1302, 2003

30. Fry M & Green DE: Cardiolipin requirement by cytochrome oxidase and the catalytic role of phospholipid. *Biochem Biophys Res Com* 93:1238-1246, 1980

31. Ohtsuka T, Nishijima M, Suzuki K & Akamatsu Y: Mitochondrial Dysfunction of a Cultured Chinese Hamster Ovary Cell Mutant Deficient in Cardiolipin. *J Biol Chem* 268:22914-22919, 1993

32. Cao J, Liu Y, Lockwood J, Burn P & Shi Y: A novel cardiolipin-remodeling pathway revealed by a gene encoding an endoplasmic reticulum-associated acyl-CoA:lysocardiolipin acyltransferase (ALCAT1) in mouse. *J Biol Chem* 279:31727-34, 2004

33. Hatch GM: Cell biology of cardiac mitochondrial phospholipids. *Biochem Cell Biol* 82:99-112, 2004

34. Ponsot E, Zoll J, N'Guessan B, Ribera F, Lampert E, Richard R, Veksler V, Ventura-Clapier R & Mettauer B: Quantitative and qualitative mitochondrial adaptations of substrates utilizations in rat cardiac and skeletal muscles. *J Cell Physiol* 203:479-486, 2005

35. Puigserver P, Wu Z, Park CW, Graves R, Wright M & Spiegelman BM: A cold-inducible coactivator of nuclear receptors linked to adaptive thermogenesis. *Cell* 92:829-839, 1998

36. Zong H, Ren JM, Young LH, Pypaert M, Mu J, Birnbaum MJ & Shulman GI: AMP kinase is required for mitochondrial biogenesis in skeletal muscle in response to chronic energy deprivation. *Proc Natl Acad Sci U S A* 99:15983-15987, 2002

37. Saks VA, Khuchua ZA, Vasilyeva EV, Belikova OY & Kuznetsov AV: Metabolic compartmentation and substrate channelling in muscle cells - Role of coupled creatine kinases in *in vivo* regulation of cellular respiration - A synthesis. *Mol Cell Biochem* 133:155-192, 1994

38. Wicks KL & Hood DA: Mitochondrial adaptations in denervated muscle: relationship to muscle performance. *Am J Physiol* 260:C841-C850, 1991

39. Schlame M, Rua D & Greenberg ML: The biosynthesis and functional role of cardiolipin. *Prog Lipid Res* 39:257-288, 2000

40. Heron C, Corina D & Ragan CI: The phospholipid annulus of mitochondrial NADH-ubiquinone reductase: a dual phospholipid requirement for enzyme activity. *FEBS Lett* 79:399-403, 1977

41. Schagger H, Hagen T, Roth B, Brandt U, Link TA & von Jagow G: Phospholipid specificity of bovine heart bc1 complex. *Eur J Biochem* 190:123-130, 1990

42. Muller M, Moser R & Cheneval DCE: Cardiolipin is the membrane receptor for mitochondrial creatine phosphokinase. *J Biol Chem* 260:3829-3843, 1985

43. Xu Y, Sutachan JJ, Plesken H, Kelley RI & Schlame M: Characterization of lymphoblast mitochondria from patients with Barth syndrome. *Lab Invest* 85:823-830, 2005

44. Jiang YJ, Lu B, Xu FY, Gartshore J, Taylor WA, Halayko AJ, Gonzalez FJ, Takasaki J, Choy PC & Hatch GM: Stimulation of cardiac cardiolipin biosynthesis by PPARalpha activation. *J Lipid Res* 45:244-252, 2004

45. Taylor WA, Xu FY, Ma BJ, Mutter TC, Dolinsky VW & Hatch GM: Expression of monolysocardiolipin acyltransferase activity is regulated in concert with the level of cardiolipin and cardiolipin biosynthesis in the mammalian heart. *BMC Biochem* 3:9, 2002

46. Han X, Yang J, Cheng H, Yang K, Abendschein DR & Gross RW: Shotgun Lipidomics Identifies Cardiolipin Depletion in Diabetic Myocardium Linking Altered Substrate Utilization with Mitochondrial Dysfunction. *Biochemistry* 44:16684-16694, 2005

FIGURE LEGENDS

Figure 1: Substrate utilization by cardiac mitochondria. Pyruvate enters the Krebs cycle by pyruvate dehydrogenase (PDH), producing acetyl-CoA (Ac-CoA). Octanoyl-carnitine undergoes β-oxidation and produces acetyl-CoA, NADH and $FADH_2$. Malate enters mitochondria through oxoglutarate/malate carrier (OMC) and produces mainly NADH by mitochondrial malate dehydrogenase (mMDH), while glycerol-3 phosphate (G3P) produces $FADH_2$ by the mitochondrial glycerol-phosphate dehydrogenase (mGDH). Succinate produces mainly $FADH_2$ that enters the respiratory chain through complex-II. NADH is reoxidized in the respiratory chain at complex-I and $FADH_2$ at complex-II.

Figure 2: Electron microscopic images of left ventricle and papillary muscles from control (A, B) and AMPKa2$^{-/-}$ (C-F) mice. (A) Overview of a control myocyte in longitudinal section, with mitochondria and myofibrils arranged in regular longitudinal columns. (C and E) Longitudinal section of cardiomyocytes from papillary (C) and ventricular (E) muscles from AMPKα2$^{-/-}$ mice showing myofibrillar disorganization, and irregular arrangement of intermyofibrillar mitochondria with clusters of mitochondria of variable size. (B) Detail of sarcomeres in a control myocyte, showing mitochondria tightly packed along sarcomeres. (D and F) Details of sarcomeres in AMPKα2$^{-/-}$ myocytes from papillary (D) and ventricular (F) muscles, showing dense packing of mitochondria of irregular size. Asterisk: large mitochondria having irregular shape. Arrows: splitting of myofibrils. Arrowhead: dividing mitochondrion.

Figure 3. A. Decreased substrate utilization by cardiac mitochondria in AMPKa2$^{-/-}$ mice. Respiration rates were measured during the cumulative addition of substrates in saponin-skinned cardiac fibers of control and AMPKα2$^{-/-}$ mice. VO_2: rate of O_2 consumption in µmol.min^{-1}.g dw^{-1}. G3P: glycerol-3-phosphate, Mal: malate, Oct: octanoyl-carnitine, Pyr: pyruvate, Glu: glutamate. * $p<0.05$ versus control. **B. Respiration rate through complex-I is specifically inhibited in AMPKa2$^{-/-}$ mouse heart.** VO_2: Rate of O_2 consumption in µmol.min^{-1}.g dw^{-}1 in saponin-permeabilized cardiac fibers. Complex-I: respiration with 2mmol/l malate and 5mmol/l glutamate. Complex-II: respiration with 10mmol/l succinate. * $p<0.05$ versus control.

Figure 4. A. Cardiolipin content is decreased in AMPKa2$^{-/-}$ mice mitochondria. Data obtained by colorimetric assay with the NAO (10-N-nonyl acridine orange) in cardiac muscle of AMPK$\alpha 2^{-/-}$ (n=6) and littermate (n=6) mice in nmoles per mg of mitochondrial proteins. * $p<0.05$ versus control. **B. Gene expression.** Real-time quantitative RT-PCR analysis of mRNA expression of peroxisome proliferator activated-receptor γ -coactivator-1α (PGC-1α), CTP:PA cytidylyltransferase (CDS2), carnitine palmitoyl transferase 1 (CPT-1), tafazzin (TAZ) and acyl-CoA:lysocardiolipin acyltransferase 1 (ALCAT1) in cardiac muscle of AMPK$\alpha 2^{-/-}$ (n=6) and littermate (n=6) mice. Results are given as means ± S.E.M. in arbitrary unit (a.u.) normalized to Cyclophilin A transcription and corrected for the amount of total RNA relative to muscle weight.

Table 1. Primers used for real-time PCR amplification

Gene	GenBank accession number	Forward Primer (5'-3') / Reverse Primer (5'-3')	PCR product size (bp)
PGC-1a	NM_008904	CACCAAACCCACAGAGAACAG GCAGTTCCAGAGAGTTCCACA	210
CDS2	NM_138651	CGGTTCATCTCCTTTGCCC GATGACGCACGAGATGGGA	201
CPT-1	NM_009948	TCACCTGGGCTACACGGAGA TCGGGGCTGGTCCTACACTT	219
TAZ	NM_181516	TTGGACGGCTGATTGCTGAG TGTGAGGGCTTTCCGCATCT	215
ALCAT1	NT_039658	GGAAGTGGAAGGATGATAAG GTTTGAGGGATGTTGTAAGG	286
CycA	NM_017101	GAGCACTGGGGAGAAAGGAT CTTGCCATCCAGCCACTCAG	259

PGC-1α: peroxisome proliferator activated receptor gamma co-activator 1α; CDS2: CTP: phosphatidic acid cytidylyltransferase 2; CPT-1: carnitine palmitoyl transferase I; TAZ: taffazin, ALCAT1: acyl-CoA:lysocardiolipin acyltransferase 1; CycA: cyclophilin A

Table 2. Functional data

	Wild type (n=5)		AMPKa2-/- (n=5)	
	glucose	**glucose+oleate**	**glucose**	**glucose+oleate**
Ventricular pressure, mmHg	87±7	109±7	85±5	118±6
Heart rate, beats/min	358±18	317±17	365±9	337±16
Rate Pressure product, RPP	2.9±0.1	3.2±0.1	2.9±0.2	3.6±0.2
+DP/dt, mmHg.sec^{-1}	3818±229	4088±264	3778±356	4533±465
-DP/dt, mmHg.sec^{-1}	-2719±187	-3053±131	-2513±153	-3167±141
Oxygen consumption rate, QO_2	6.4±0.7	8.6±0.7*	6.0±0.6	8.0±1.0
QO_2/RPP	2.3±0.3	2.7±0.3	2.1±0.3	2.3±0.3

Hearts were first perfused with glucose 11 mM and then with glucose 5 mM and 0.4 mM oleate. Values are means ± S.E.M., n = number of mice; RPP: 10^4.mmHg.beats.min^{-1}. QO_2: µmol O_2.min^{-1}.g^{-1} ww. No statistical difference between control and AMPK$\alpha 2^{-/-}$. * $p < 0.05$, glucose versus glucose + oleate.

Table 3. Energy metabolism of cardiac fibers

	Control	AMPKa2$^{-/-}$
Morphometric data		
Number of hearts	3	3
Total mitochondria	36.1±1.8	37.6±0.5
SS mitochondria	3.9±0.4	11.3±1.1*
IM mitochondria	32.2±1.4	26.3±1.4*
Mitochondrial function		
Number of fibers	20	18
V_0, µmoles O_2/min/g dw	3.0±0.3	2.7±0.2
Vglu+mal, µmoles O_2/min/g dw	18±1	13±1*
Vsuc, µmoles O_2/min/g dw	19±2	23±2
Vsuc/Vglu+mal	1.2±0.1	1.7±0.2*
Vduroq*, µmoles O_2/min/g dw	50±10	54±8
Km_{ADP}	253±54	289±49
Km_{Cr}	73±14	52±11
ACR	6.2±0.9	4.9±0.4
Enzymatic Activity (IU/mg prot)		
Number of animals	9	8
Citrate synthase	836±58	742±48
Cytochrome oxidase	1207±120	1114±114
Creatine kinase (CK)	2637±182	2860±171
mi-CK	653±96	716±67
Adenylate kinase	2107±150	2414±219
Lactate dehydrogenase	932±75	999±70
Complex-I (decyl-ubiquinone)	450±64	413±51
Complex-I (ferricyanure)	990±86	914±77
Complex-II	264±27	226±21
Malate dehydrogenase (MDH)	5906±500	5843±573
Mitochondrial MDH	1913±250	1818±112

Values are means ± S.E.M., nd: not detectable. Morphological data are expressed in % cell volume. Oxygen consumption rates in the absence (V_0) and presence of 2mmol/l ADP (Vglu+mal respiration through complex I with glutamate+malate; Vsuc respiration through complex II with succinate,); Vduroq respiration through complex III with reduced duroquinol *(n=10 for each). Michaelis-Menten constant of respiration rate for ADP (µmol/l) without (Km) or with (Km_{Cr}) 20mmol/l creatine. ACR: acceptor control ratio (Vglu+mal/V_0). * $p < 0.05$, versus control mice.

Table 4. Fatty acid composition of cardiac lipids

Fatty acid	COMPOSITION (%)					
	Heart Mitochondria		Heart Phospholipids		Non phosphorous Lipids	
	Control	AMPKa2$^{-/-}$	Control	AMPKa2$^{-/-}$	Control	AMPKa2$^{-/-}$
16:0	13.4±0.6	14.6±0.7	14.2±0.9	16.4±0.5	19.8±0.5	18.1±0.4
16:1 w9	1.1±0.2	1.0±0.3	0.3±0.1	0.35±0.03	6.2±0.7	4.5±0.3
18:0	18±1	17±1	21±1	21±1	8.9±0.3	9±1
18:1 w9	6.7±0.3	7.0±0.2	6.3±0.3	6.3±0.3	19.0±0.4	22.0±0.4*
18:1 w7	2.51±0.03	2.7±0.1	2.26±0.04	2.5±0.1	1.4±0.1	1.5±0.3
18:2 w6 LA	19.2±0.6	16.8±0.4*	18.0±0.2	16.3±0.5*	20.1±1.5	24.3±0.3*
20:4 w6	4.5±0.2	4.3±0.2	5.2±0.2	4.9±0.3	3.0±0.1	2.6±0.4
22:5 w3	1.02±0.03	1.2±0.1	1.1±0.1	4.1±3.1	1.5±0.1	1.5±0.4
22:6 w3	30±2	31±2	28±2	24±1	5.1±0.4	5.4±0.6
SFA	32±1	33±1	36±2	34±5	36±1	39±5
MUFA	12±1	11±1	9.7±0.3	9±1	31±1	36±6
PUFA w6	25.1±0.5	22.5±0.6*	25.2±0.4	20±3	25±1	33±5
PUFA w3	31±2	33±2	29±2	24±4	8.1±0.3	9±1

Values are means ± S.E.M. *, $p<0.05$. SFA: saturated fatty acids. MUFA, mono-unsaturated fatty acids. PUFA: polyunsaturated fatty acids. LA, linoleic acid. Three control and three AMPK$\alpha 2^{-/-}$ mice were used.

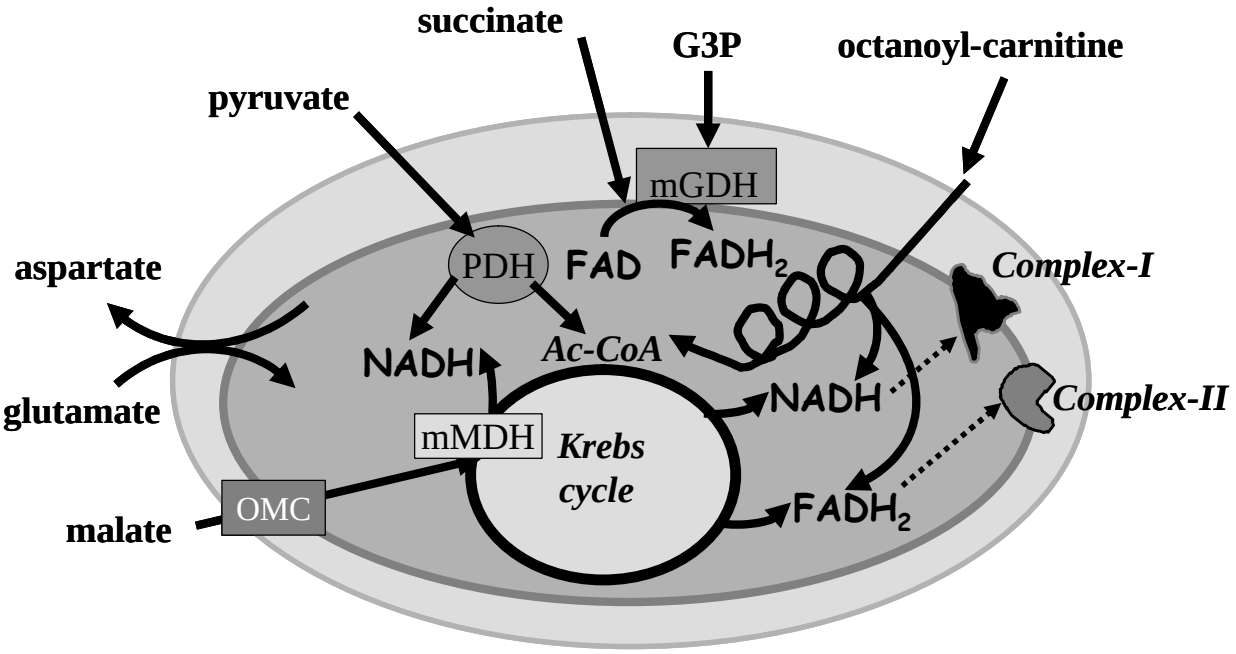

Figure 1

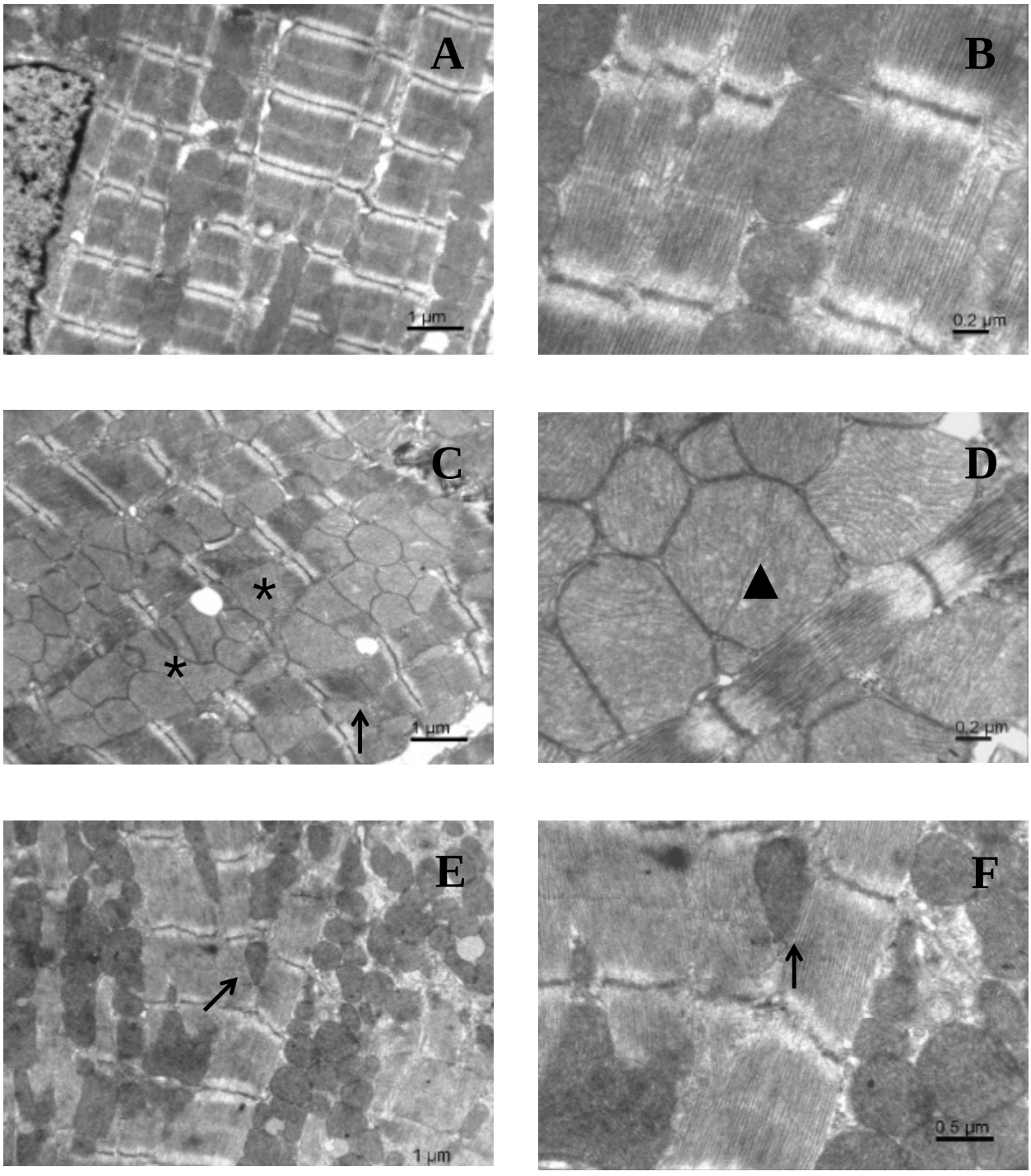

Figure 2

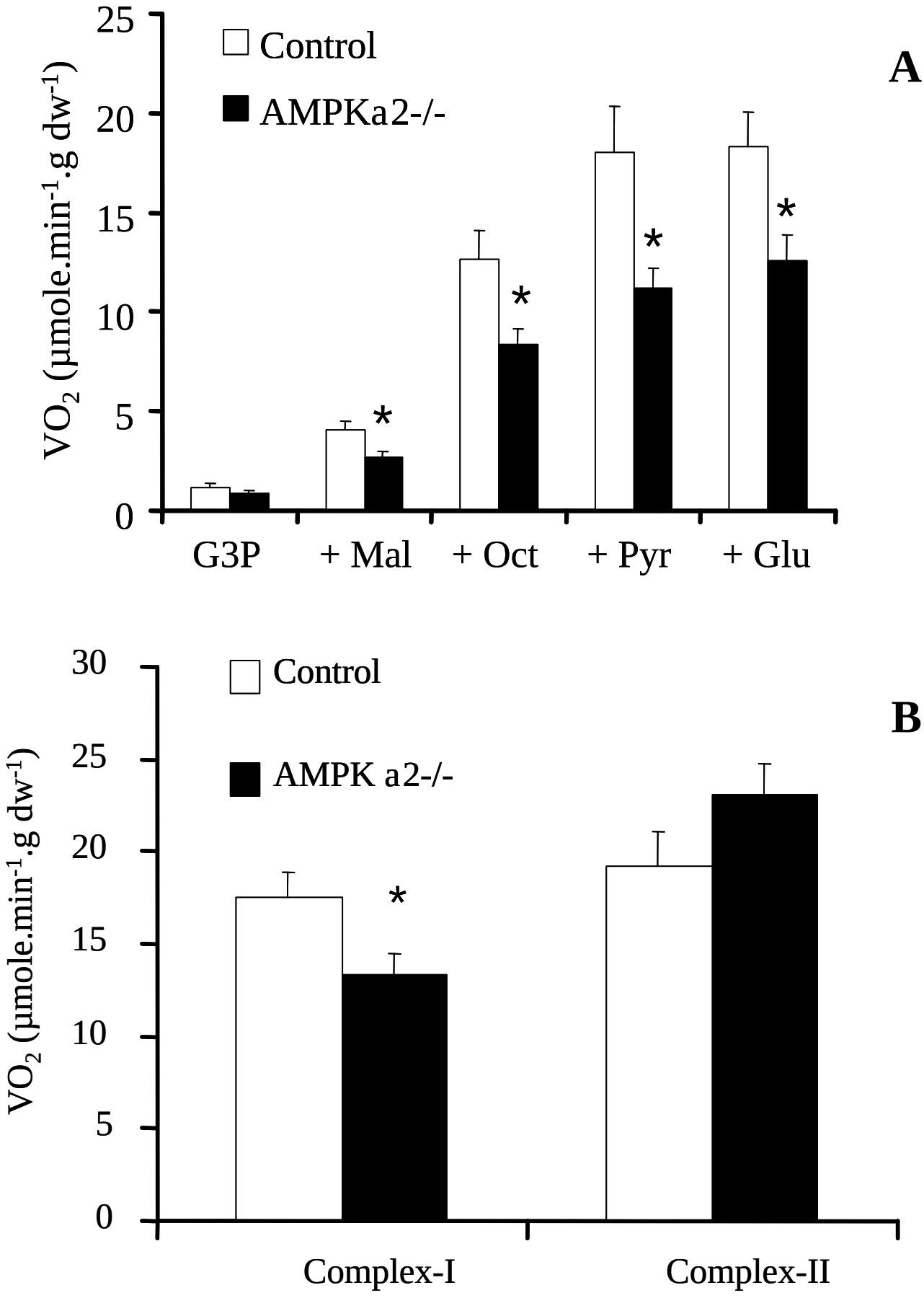

Figure 3

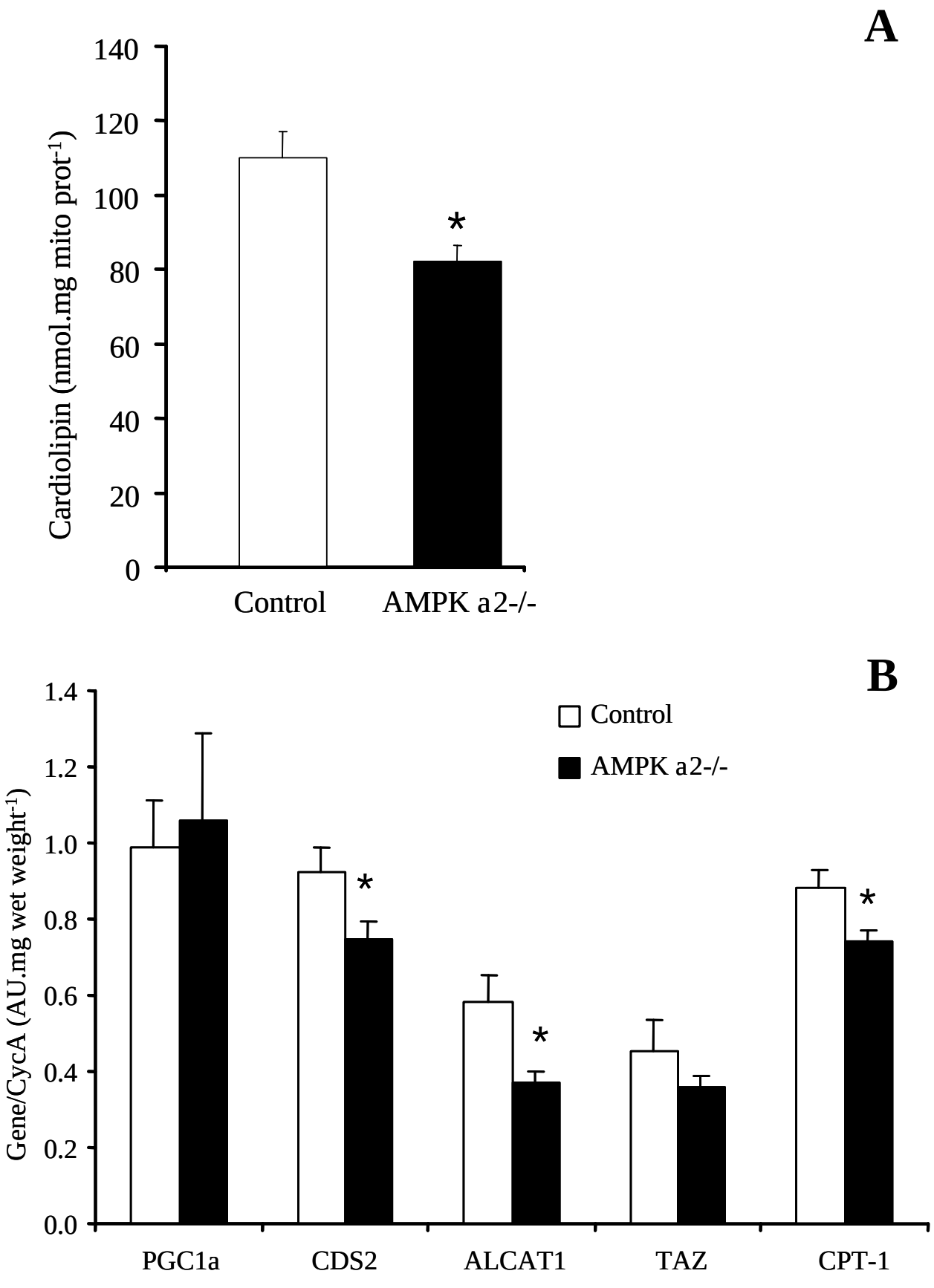

Figure 4